

Corrosion Response of Twin Roll Cast AZ31 Alloy in Biologically Relevant Environments

Tanay Bag^{1*}, Dr. Amrut Agasti², and Dr. Rajesh Khatirkar²

¹Visvesvaraya National Institute of Technology, Interdisciplinary Board (Biomedical Engineering), Nagpur-440010, Maharashtra, India

²Visvesvaraya National Institute of Technology, Department of Metallurgical and Materials Engineering, Nagpur-440010, Maharashtra, India

Abstract. The present work highlights twin-roll cast (TRC) AZ31 magnesium alloy as an energy-saving processing alternative to conventional ingot-cast AZ31 magnesium alloy through analytical characterization, corrosion behaviour in in-vitro biologically relevant environments for degradable implant applications. Conventional AZ31 magnesium alloy is a standard lightweight and bone-matching alloy for implants, it is still far from field applications due to rapid corrosion, hydrogen buildup under physiological conditions, and pitting corrosion. The present study focuses solely on the microstructural characteristics and not the cytotoxic effect of the TRC AZ31 magnesium alloy. 0.9% NaCl and Ringer's solution were used to identify the role of the diffusion layer over pitting, while simulated body fluid (SBF) was used for mimicking in-vitro physiological conditions that curb pitting and hydrogen evolution. Potentio-dynamic polarization was used to study the corrosion behaviour, hydrogen evolution studies were done, micro-hardness testing was performed for microstructure comparison, secondary electron microscopy was implemented to understand the diffusion barrier formation, and energy-dispersive X-ray spectroscopy was used for elemental analysis. Overall, these insights show how microstructure, environment, and corrosion interact, for broader biomedical adoption of AZ31 alloy.

1 Background

For designing biodegradable implants, magnesium-based alloys are grabbing a lot of attention for their promising features like good strength-to-weight ratio, biocompatibility, and a density comparable to that of cortical bone (1.8–2.1 g/cm³) [1, 2], but the hexagonal close-packed (HCP) crystal structure at room temperature makes their processing a significant manufacturing challenge. Early failure from strain localization or crack development during deformation makes the magnesium alloys processing difficult and calls for specialized processing routes with improved formability. However, these approaches not only increase the manufacturing complexity and costs but also limit industrial applicability. Recent advancements in twin-roll cast (TRC) processing for magnesium alloys enable a cost-effective, energy-efficient, non-porous sheet production with comparatively lower segregation than ingot casting [3]. Among these, AZ31 magnesium alloy was specifically chosen as the subject of this study because it is the most extensively characterized magnesium alloy, offers an optimal cost-strength-corrosion balance, making it suitable for the biomedical applications.

Magnesium alloys undergo a highly dynamic and complex degradation process in vivo due to the presence of electrolytes, organic compounds, and proteins, influencing corrosion kinetics by modifying the electrochemical environment. Moreover, released magnesium ions elicit distinct host responses during multi-staged bone healing process as an essential element in the bone matrix and as a key secondary

messenger in the intracellular signalling pathway [4]. Hence, excessive release of magnesium ion not only causes hypermagnesemia, an elevated level of magnesium ions in the plasma, but also simultaneously raises the production of hydrogen gas that rapidly diffuses into the surrounding tissue, which can impair tissue repair [5, 6]. Therefore, the aim of the present work is to study the microstructure and short-term in-vitro corrosion behaviour of TRC AZ31 magnesium alloy in different biologically relevant media, while restricting biological compatibility assessments.

2 Experimental Procedure

The present study utilized the twin-roll cast (TRC) AZ31 magnesium alloy, whose element composition is detailed in Table 1. The Mg alloy sheet samples were metallographically polished in steps up to 2500 silicon carbide grit paper, followed by polishing with 0.05 µm alumina suspension in 99.5% ethanol-based lubricant followed by final micro-polishing with cloth. Samples were etched using an acetic picral solution for optical microscopy (Zeiss, Germany) analysis [7]. The grain size distribution was determined using ImageJ software [8]. For micro-hardness measurement, a micro-hardness tester (Mitutoyo, Japan), was used and Vickers hardness number was obtained using a load of 100 g. 10 readings were taken at different locations after polishing the alloy surface. To understand the hydrogen evolution, the specimens were immersed in biofluid, i.e., 0.9% NaCl solution, Ringer's solution, and simulated body fluid (SBF), for approximately 3 hours at 37±0.2°C. Hydrogen evolution tests were conducted with n=5 replicates per biofluid condition. Volume measurements

*Corresponding author: tanay666bag@tuta.io

used graduated cylinders (0.01 ml precision) with automated data logging every 5 minutes. This 3-hour duration specifically targeted the critical initial hydrogen evolution burst (>70% gas release within the first 60 minutes), which represents the dominant corrosion kinetics phase and primary clinical concern for acute tissue disruption in early implant stages. Following the corrosion tests, the morphology of the corroded surfaces was analysed by scanning electron microscopy (SEM) coupled with energy-dispersive X-ray spectroscopy (EDS) to determine the elemental composition.

Table 1. Alloying element composition (wt%) of TRC AZ31 magnesium alloy sheet

Al	Zn	Mn	Ca	Si	Cu
3.0	1.0	0.5	0.04	0.1	0.01

2.1 Selection and Preparation of biofluids

In this work, three different biofluids, namely 0.9% NaCl solution, Ringer’s solution, and simulated body fluid (SBF), were selected to represent simplified and physiologically relevant corrosion environments for magnesium alloy (AZ31). The 0.9% NaCl solution was used as a baseline chloride-containing medium to study the effect of aggressive ions on general and pitting corrosion. Ringer’s solution, containing Na⁺, K⁺, Ca²⁺ and Cl⁻ ions, was chosen to better mimic the inorganic electrolyte composition of extracellular body fluids in clinical conditions. SBF was selected to simulate the ionic composition of human blood plasma, especially with respect to Ca²⁺ and PO₄³⁻ ions and is commonly recommended in standards and literature for in-vitro evaluation of biomaterials.

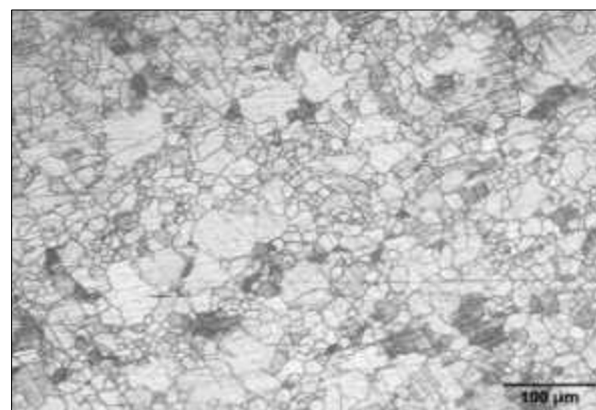
All solutions were prepared according to standard procedures reported in the literature and following the ionic concentration guidelines given in relevant ISO standards for biological evaluation of medical devices (e.g., ISO 10993 series) and simulated physiological solutions. The SBF solution was prepared by dissolving reagent-grade salts in deionized water in a controlled order under continuous stirring, and the pH was adjusted to 7.40 ± 0.05 at 37 °C using tris-(hydroxymethyl)-aminomethane and hydrochloric acid to match physiological conditions. The use of these three biofluids therefore allows the comparison of TRC AZ31 corrosion behaviour in a simple chloride medium, a clinically relevant electrolyte solution, and a more physiologically representative fluid with ionic composition like human plasma.

3 Results and Discussion

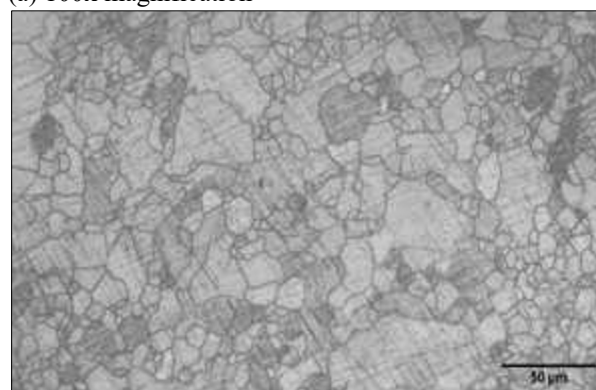
3.1 Grain Size Analysis

The microstructure of TRC AZ31 magnesium alloy under the optical microscope (OM) revealed a bi-modal grain distribution (Fig. 1), indicating a mixture of fine and coarse grains with an average grain size of 41.41 μm. It is generally considered that defects like grain

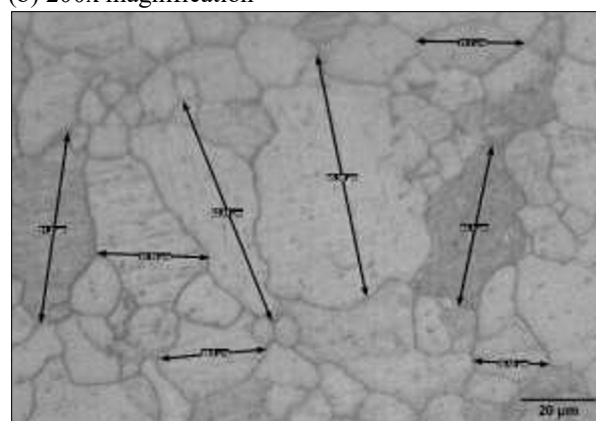
boundaries, twins and dislocations are the preferred sites for corrosion due to their higher electrochemical activity. Due to the presence of finer grains, more grain boundaries are expected, suggesting improved alloy strength and ductility, but these high-energy sites are also responsible for initiating and propagating corrosion, particularly in aggressive biological environments. Some studies [10–12] have also suggested that secondary processing like annealing of TRC AZ31 magnesium alloy can improve the grain homogeneity, resulting in enhanced corrosion resistance.



(a) 100x magnification



(b) 200x magnification



(c) 500x magnification

Fig. 1. Optical micrographs of twin-roll cast (TRC) AZ31 magnesium alloy at different magnifications.

3.2 Microhardness Analysis

Microhardness assesses the localized mechanical resistance to deformation, which is especially important for heterogeneous structures. After performing Vickers hardness testing with a 100 g load, the microhardness values were found to range between 50 and 60 HV. These values were obtained by performing measurements at five different locations on the polished surface to account for microstructural variations. The TRC process leads to a finer grain size compared to conventional casting, suggesting an improvement in local strength and ductility. However, microhardness testing only provides information about the local resistance to indentation, and additional mechanical tests such as tensile and fatigue measurements are required to fully establish the mechanical performance of TRC AZ31 for implant applications.

3.3 Hydrogen Evolution Profile Analysis

Hydrogen evolution was monitored using a customized water displacement setup (Fig. 2), in which the hydrogen generated during corrosion displaced water in an inverted graduated cylinder, allowing direct volume measurements of the released gas over time. The evolution rate provides a direct measure of TRC AZ31 corrosion kinetics during 3-hour immersion tests ($n = 5$ replicates) at 37 ± 0.2 °C in 0.9% NaCl, Ringer's solution, and simulated body fluid (SBF). Gas release peaked during the initial biofluid contact (>70% within the first hour) and then followed a diffusion-controlled decline (Fig. 3). Mean hydrogen evolution rates \pm SD remained below 10^{-4} ml·cm⁻²·s⁻¹ across all conditions (Table 2), with ANOVA confirming significant differences between the biofluids ($F(2,12) = 18.4$, $p < 0.001$; 0.9% NaCl > Ringer's solution > SBF).

SEM analysis revealed uneven, porous corrosion films in 0.9% NaCl and Ringer's solution, correlating with the elevated hydrogen evolution in these media, whereas more uniform and compact layers were observed in SBF. These surface films act as diffusion barriers that control the subsequent degradation kinetics, with SBF promoting relatively stable, hydroxyapatite-like protective layers. The decay of the hydrogen evolution rate after the initial burst can be qualitatively described by a simple diffusion-controlled behaviour.

Table 2. Hydrogen evolution rates of TRC AZ31 magnesium alloy during 3-hour immersion at 37 ± 0.2 °C ($n = 5$)

Biofluid	Surface area of alloy (cm ²)	H ₂ rate (ml·cm ⁻² ·s ⁻¹)	SD (×10 ⁻⁴)
0.9% NaCl sol.	4.75	1.7544×10^{-4}	± 0.12
Ringer's sol.	4.345	6.4×10^{-4}	± 0.08
SBF	3.525	1.182×10^{-5}	± 0.10

3.4 Corrosion Analysis

Potentiodynamic polarization (Tafel) tests followed ASTM G59-97(2014) on polished samples. A three-

electrode cell used: TRC AZ31 working electrode, Pt wire counter, Ag/AgCl. From Table 3, it can be observed that the corrosion rate of TRC AZ31 magnesium alloy (Fig. 4) is slightly higher than the reported corrosion rate of conventionally cast AZ31 alloy. From Table 3, it can be observed that the corrosion rate of TRC AZ31 magnesium alloy (Fig. 4) is slightly higher than the reported corrosion rate of conventionally cast AZ31 alloy. The higher corrosion rate may arise due to the bi-modal distribution of grains and the relatively higher fraction of grain boundaries, which are supposed to be the main sites for corrosion initiation and propagation.



Fig. 2. Schematic of the customized water displacement setup used for hydrogen evolution measurements.

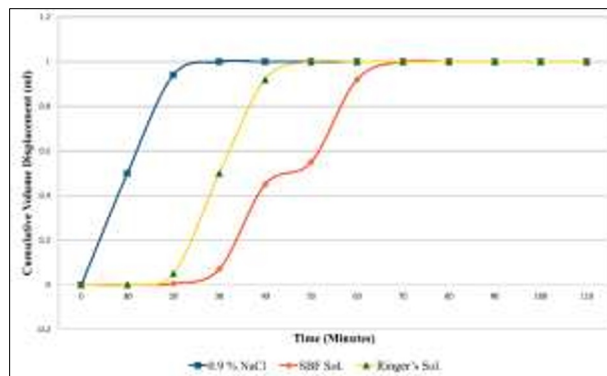


Fig. 3. Hydrogen evolution rate with respect to time

The corrosion rate of TRC AZ31 magnesium alloy is generally determined from the corrosion current density (I_{corr}) derived from the Tafel polarization curve using the following formula in terms of mils per year (mpy).

$$CR \text{ (mpy)} = \frac{0.13 \times I_{corr} \times E_w}{n \cdot \rho} \quad (1)$$

I_{corr} is the corrosion current density in $\mu\text{A} \cdot \text{cm}^{-2}$, E_w is the equivalent weight of the TRC AZ31 alloy, n is the number of electrons exchanged in the corrosion reaction, and ρ is the density of the alloy in $\text{g} \cdot \text{cm}^{-3}$. The corrosion rate in $\text{mm} \cdot \text{year}^{-1}$ was obtained by converting mpy using the following relation,

$$1 \text{ mpy} = 0.0254 \text{ mm} \cdot \text{year}^{-1} \quad (2)$$

Table 3. Corrosion rate comparison between TRC and ingot cast AZ31 magnesium alloy

Biofluid	I_{corr} ($\mu A \cdot cm^{-2}$)	Corrosion rate (mm/year)	Corrosion rate of TRC AZ31 in mpy	Reported corrosion rate of ingot cast in mpy
0.9% NaCl	970	10.35	407.48	400 [15]
Ringer's	50	0.533	21	307 [15]
SBF	334	3.55	139.76	20.21 [16]

The calculated corrosion rates of TRC AZ31 in different biofluids and the reported corrosion rates of conventional AZ31 from the literature are summarized in Table 3. It should be noted that the comparison with conventional AZ31 is based on reported literature values and not on parallel experiments in the present work, so this comparison is indicative rather than definitive.

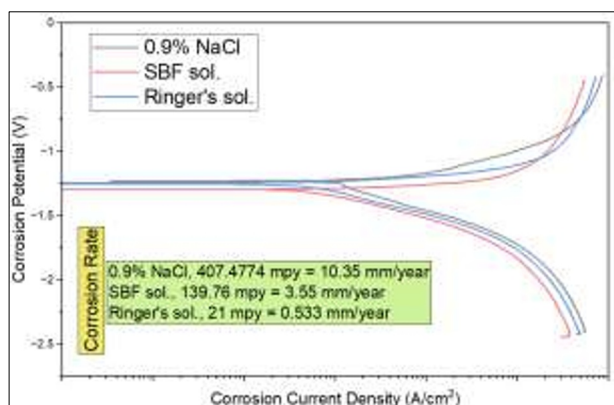
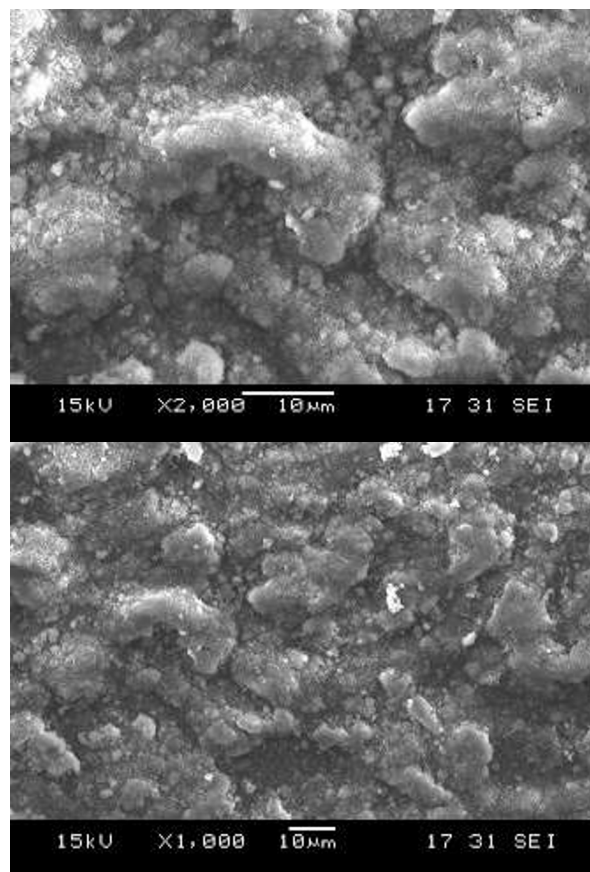


Fig. 4. Corrosion rate determined from corrosion current density (I_{corr}) value derived from Tafel polarization curve

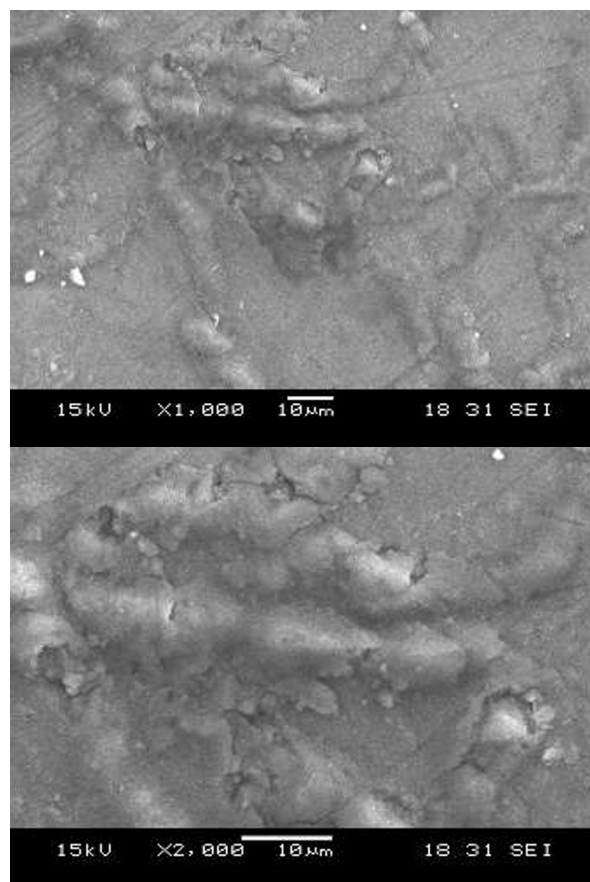
3.5 Morphological and Elemental Analysis

3.5.1 Secondary Electron Microscopy (SEM)

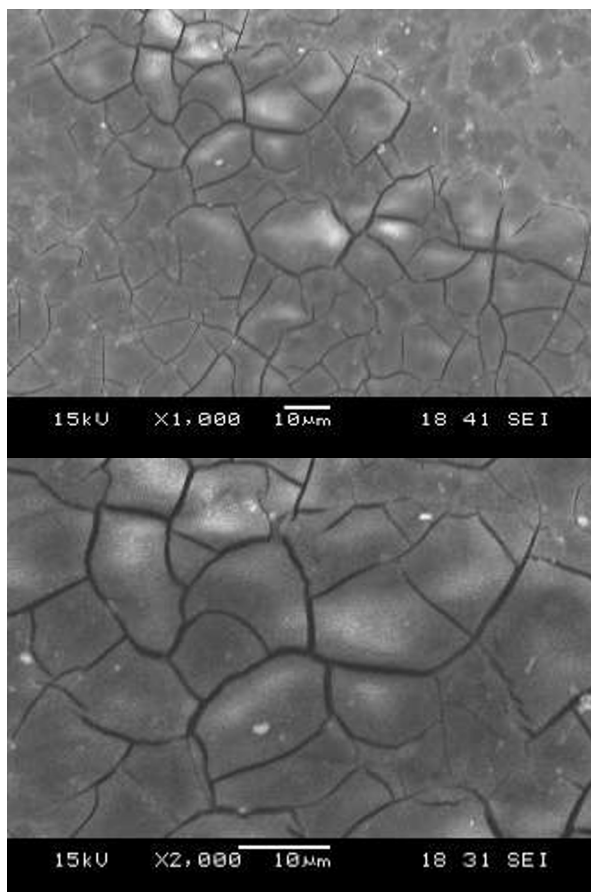
The surface morphology of TRC AZ31 magnesium alloy (Fig. 5) after 3-hour immersion in 0.9% NaCl solution, Ringer's solution, and SBF was examined by SEM to identify the dominant corrosion features in each biofluid. Specimens exposed to 0.9% NaCl solution (Fig. 5a) showed a rough and uneven surface with pronounced localized attack and porous corrosion products, indicating severe pitting and unstable surface film formation. In Ringer's solution (Fig. 5b), the corrosion morphology remained heterogeneous, with a combination of shallow pits and partially cracked surface layers, suggesting intermediate stability of the corrosion products. In contrast, specimens immersed in SBF (Fig. 5c) exhibited comparatively smoother and more uniform surfaces covered with compact corrosion layers, indicating the formation of more stable protective films in this medium.



(a) Surface morphology after 0.9% NaCl immersion.



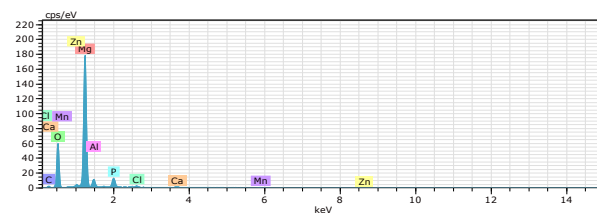
(b) Surface morphology after Ringer's solution immersion.



(c) Surface morphology after SBF immersion.
 Fig. 5. Corrosion morphology under SEM

3.5.2 Energy-dispersive X-ray Spectroscopy (EDS) Analysis

EDS analysis was used to qualitatively assess the elemental composition of the corrosion products formed on the TRC AZ31 surface in different biofluids. Although the present EDS analysis is qualitative and does not provide precise phase identification, these observations support the conclusion that SBF promotes more compact and protective surface films compared to 0.9% NaCl and Ringer’s solution, in agreement with the lower hydrogen evolution rates and corrosion kinetics observed in this medium.



(c) EDS of alloy surface after SBF immersion
 Fig. 6. EDS spectra of TRC AZ31 magnesium alloy surface for different biofluids.

4 Conclusions

The twin-roll cast (TRC) AZ31 magnesium alloy is a cost-effective manufacturing route with a refined microstructure and promising local mechanical response (microhardness 50–60 HV) compared to conventionally cast AZ31 alloy. The short-term in-vitro corrosion tests in 0.9% NaCl, Ringer’s solution, and SBF show hydrogen evolution rates below $10^{-4} \text{ ml}\cdot\text{cm}^{-2}\cdot\text{s}^{-1}$ and corrosion rates of the same order of magnitude as reported values for conventionally cast AZ31, indicating that TRC processing does not introduce severe deterioration in early-stage corrosion behaviour. At the same time, the bi-modal grain structure and high grain boundary density still contribute to considerable corrosion susceptibility, which limits the direct use of TRC AZ31 as an implant material without further optimization.

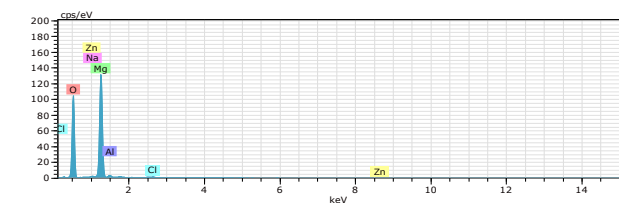
The present work is restricted to microstructural characterization, microhardness measurements, and short-term in-vitro corrosion evaluation, and does not include comprehensive mechanical testing (such as tensile or fatigue) or any biological compatibility or cytotoxicity assessment. Therefore, no definitive conclusions can be drawn regarding the overall mechanical performance or clinical suitability of TRC AZ31 for biomedical implants. Future research should focus on combining TRC processing with appropriate surface modification or coating strategies, as well as systematic long-term in-vitro and in-vivo studies, including mechanical and biological evaluations, to extend the functional lifespan of TRC AZ31 while maintaining its biodegradability and to properly assess its potential for biomedical applications.

Acknowledgements

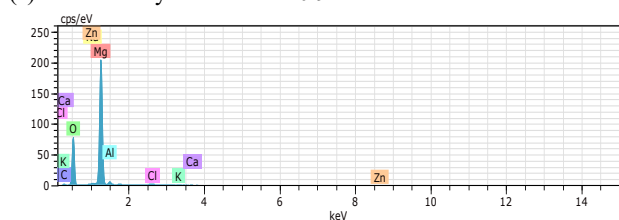
The authors would like to thanks The Director, VNIT, Nagpur for providing the facilities and constant encouragement to publish this work.

Conflict of Interest

The authors declare that there is no conflict of interest of any sort between the authors or with others regarding the work presented.



(a) EDS of alloy surface after 0.9% NaCl sol. Immersion.



(b) EDS of alloy surface after Ringer’s sol. immersion

References

Journal articles

1. J. Alias, N. Mohamed, M. Ishak, X. Zhou, G. Thompson, The Influence of Hot Forming on the Microstructure and Corrosion Behaviour of AZ31B Magnesium Alloys. *Indonesian Journal of Science and Technology*. **3**, 2 (2018).
<https://doi.org/10.17509/ijost.v3i2.12758>
2. H. Gerengi, Cabrini, Marina, Solomon, M. Moses, Kaya, Ertugrul, Gritti, Luca, Yola, L. Mehmet, Chemical, Electrochemical, and Surface Morphological Studies of the Corrosion Behavior of the AZ31 Alloy in Simulated Body Fluid: Effect of NaOH and H₂O₂ Surface Pretreatments on the Corrosion Resistance Property. **7**, 30 (2022)
<https://doi.org/10.1021/acsomega.2c02998>
3. K. Kittner, C. Kaden, M. Ullmann, et al., Production of AZ80 magnesium alloy wires: influence of heat treatment on microstructure and properties after twin-roll casting. *Prod. Eng. Res. Devel.* **19**: 295–306 (2025)
<https://doi.org/10.1007/s11740-024-01310-1>
4. W. Li, W. Qiao, X. Liu, D. Bian, D. Shen, Y. Zheng, J. Wu, K. Y. H. Kwan, T. M. Wong, K. M. C. Cheung, K. W. K. Yeung, Biomimicking Bone–Implant Interface Facilitates the Bioadaptation of a New Degradable Magnesium Alloy to the Bone Tissue Microenvironment. *Adv. Sci.* **8**, 23 (2021)
<https://doi.org/10.1002/advs.202102035>
5. J. Kuhlmann, I. Bartsch, E. Willbold, S. Schuchardt, O. Holz, N. Hort, D. Höche, W. R. Heineman, F. Witte, Fast escape of hydrogen from gas cavities around corroding magnesium implants. *Acta Biomaterialia*. **9**, 10 (2013)
<https://doi.org/10.1016/j.actbio.2012.10.008>
6. C. Rössig, N. Angrisani, P. Helmecke, S. Besdo, Jan-Marten Seitz, B. Welke, N. Fedchenko, H. Kock, J. Reifenrath, In vivo evaluation of a magnesium-based degradable intramedullary nailing system in a sheep model. *Acta Biomaterialia*. **25**, 369-383 (2015)
<https://doi.org/10.1016/j.actbio.2015.07.025>
7. S. Samberger, T. Kremmer, L. Stemper, S. Tourey, J. P. Uggowitzer, S. Pogatscher, Metallographic Etching of Al–Mg–Zn–(Cu) Crossover Alloys. *Adv. Eng. Mater.*, **26** (2024)
<https://doi.org/10.1002/adem.202400576>
8. A. Ercetin, F. Akkoyun, E. Şimşir, Y. D. Pimenov, K. Giasin, P. M. C. Gowdru, A. Lakshmikanthan, A. Wojciechowski. Image Processing of Mg-Al-Sn Alloy Microstructures for Determining Phase Ratios and Grain Size and Correction with Manual Measurement. *Materials*. **14**, 17 (2021)
<https://doi.org/10.3390/ma14175095>
9. Guang-Ling Song and Z. Xu. Effect of microstructure evolution on corrosion of different crystal surfaces of AZ31 Mg alloy in a chloride containing solution. *Corrosion Science*. **54**: 97-105 (2012)
<https://doi.org/10.1016/j.corsci.2011.09.005>
10. A. Tripathi and I. Samajdar and J.F. Nie and A. Tewari. Study of grain structure evolution during annealing of a twin-roll-cast Mg alloy. *Materials Characterization*. **114**: 1044-5803. (2016)
<https://doi.org/10.1016/j.matchar.2016.02.019>
11. F. Zhou and S. S. Lu and B. Jiang and R.G. Song. Effect of annealing treatment of hot-rolled AZ31 magnesium alloy on properties and stress corrosion resistance of MAO coatings. *Anti-Corrosion Methods and Materials*. **71**, 4: 403-416 (2024)
<https://doi.org/10.1108/ACMM-01-2024-2954>
12. F. Ning, Q. Le, S. Kong. Effect of annealing temperature on corrosion properties of rolled AZ31-Ce magnesium alloy. *SN Appl. Sci.* **2**, 762 (2020)
<https://doi.org/10.1007/s42452-020-2398-8>
13. Fakhri, B. Noora, Abbass, K. Muna, Hanoon, M. Mahdi, Improvement the Microstructure and Mechanical Properties of AZ31 Magnesium Alloy using Stir Friction Processing. *IOP Conference Series: Earth and Environmental Science*. **1507**, 1 (2025)
<https://doi.org/10.1088/1755-1315/1507/1/012090>
14. M. Moses, M. Ullmann, U. Prah. Twin-Roll Casting as a Grain Refinement Method and Its Influence on the Microstructure and Deformation Behavior of an AZ31 Magnesium Alloy Wire. *Crystals*. **13**, 10: 1409 (2023)
<https://doi.org/10.3390/cryst13101409>
15. Yavuzyeğit, Berzah, Karali, Aikaterina, De Mori, Arianna, Smith, Nigel, Usov, Sergey, Shashkov, Pavel, Bonithon, Roxane, Blunn, Gordon. Evaluation of Corrosion Performance of AZ31 Mg Alloy in Physiological and Highly Corrosive Solutions. *ACS Applied Bio Materials*. **7**, 3: 1735-1747 (2024)
<https://doi.org/10.1021/acsabm.3c01169>
16. U. Masood Chaudry, A. Farooq, A. Malik, M. Nabeel, M. Sufyan, A. Tayyeb, S. Asif, A. Inam, A. Elbalaawy, E. Hafez, Tea-Sung Jun, K. Hamad. Biodegradable properties of AZ31-0.5Ca magnesium alloy. *Materials Technology*. **37**, 12: 2230 – 2241. (2022)
<https://doi.org/10.1080/10667857.2021.2022571>